

Near-field scanning microwave microscope with 100 μm resolution

C. P. Vlahacos, R. C. Black,^{a)} S. M. Anlage,^{b)} A. Amar, and F. C. Wellstood
Center for Superconductivity Research, Department of Physics, University of Maryland, College Park, Maryland 20742-4111

(Received 25 June 1996; accepted for publication 6 September 1996)

We describe the operation of a simple near-field scanning microwave microscope with a spatial resolution of about 100 μm . The probe is constructed from an open-ended resonant coaxial line which is excited by an applied microwave voltage in the frequency range of 7.5–12.4 GHz. We present images of conducting structures with the system configured in either receiving or reflection mode. The images demonstrate that the smallest resolvable feature is determined by the diameter of the inner wire of the coaxial line and the separation between the sample and probe. © 1996 American Institute of Physics. [S0003-6951(96)01047-9]

Ash and Nichols¹ were the first to demonstrate a near-field scanning microwave microscope. At a frequency of 10 GHz, they obtained microwave images with $\lambda/60$ resolution, thereby showing that the diffraction limit could be breached via the use of evanescent waves. Since this initial work, near-field imaging has been accomplished in a variety of instruments which cover frequencies spanning the microwave to optical bands.^{2–6} Evanescent fields in the microwave region have been generated using the open end of a transmission line,^{7,8} a small hole in a waveguide,⁹ or a microstrip resonator.¹⁰ In this letter, we report on a simple near-field scanning microscope which operates in the 7.5–12.4 GHz range with a spatial resolution of about 100 μm , corresponding to $\lambda/360$ at 12 GHz.

In our system, the near-field probe is formed by a small open rigid coaxial probe which is connected to the end of a segment of coaxial transmission line [see Fig. 1(a)]. When a voltage is applied to the far end of the line, an electric field appears at the open end, with the most intense fields being generated near the inner conductor. The spatial extent of this field sets a lower limit on the spatial resolution, rather than the microwave wavelength. Very close to the end of the probe, the field is roughly uniform over the exposed area of the inner conductor (neglecting field enhancement at the edges), while far from the conductor the field falls inversely with distance in the radiation limit. Thus the spatial resolution of the instrument will be approximately equal to the diameter of the inner conductor, provided that it is brought closer than this to a sample.

Our experimental arrangement is shown in Fig. 1(a). A Wavetek 955 microwave source is connected to the input port of a Miteq directional coupler, the short coaxial probe is connected to a second port, and the reflection port is connected to a microwave diode detector. With this arrangement, the diode produces a dc output voltage which is proportional to the magnitude of the reflected microwave radiation. The diode output is amplified and monitored with an analog-to-digital (A/D) board which is mounted in a personal computer. The probe is made from a 50 Ω SMA connector to which is attached a short (about 10 mm long) open section of semirigid 50 Ω coaxial cable. The probes have an

outer jacket of stainless steel, a center conductor of silver-plated copper wire, and a Teflon dielectric. We have used several different probes, made from coaxial cables with the following inner (outer) conductor diameters: 480 (2130), 200 (810), and 100 (450) μm .

To generate an image, we use a micrometer-based scanning table to move the sample under the probe tip while monitoring the reflected microwave signal from the diode. The computer controls the positioning of the sample, records the output, and converts the resulting data into a false color or gray scale image.

Our system can be modeled as a resonant coaxial transmission line of total length L with a capacitor C_x at one end and a mismatched microwave supply voltage $V(\omega)$ at the other [see Fig. 1(b)]. Here C_x is the capacitance between the sample and the inner conductor of the probe. Ultimately, it is

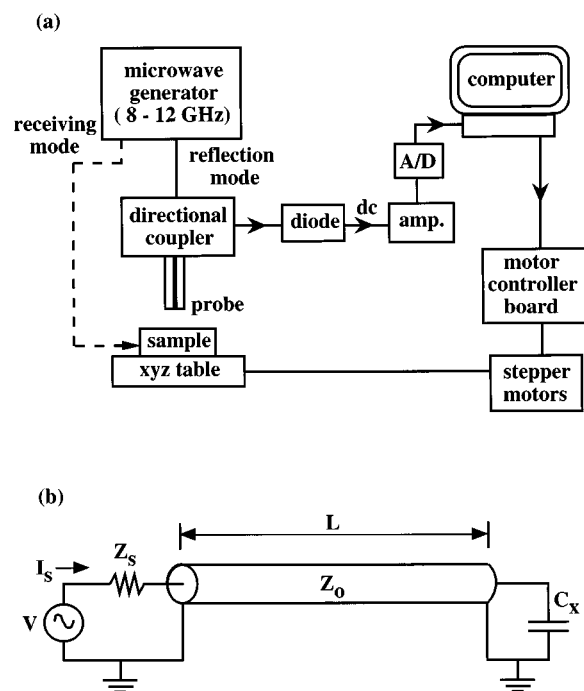


FIG. 1. Near-field scanning microwave microscope. (a) Electrical schematic, (b) experimental setup. In reflection mode the microwave output is connected to the system with a solid line, in receiving mode it is connected with dashed line.

^{a)}Present address: Quantum Design, San Diego, CA 92121-1311.

^{b)}Electronic mail: anlage@squid.umd.edu

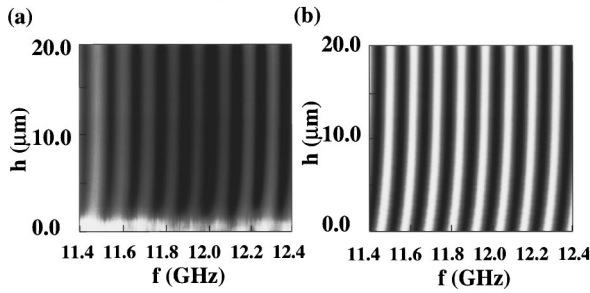


FIG. 2. Gray scale image showing reflected voltage vs height and frequency over a stainless steel sample; (a) experimental data, and (b) calculated image.

the dependence of C_x on position which leads to contrast in the reflected image. using standard transmission line theory,¹¹ the reflected voltage V is

$$|V_-| = \frac{|V(\omega)|}{\left| \left(1 + \frac{Z_s}{Z_0} \right) \left(\frac{1 + i\omega C_x Z_0}{1 - i\omega C_x Z_0} \right) e^{-2ikL} + \left(1 - \frac{Z_s}{Z_0} \right) \right|} \quad (1a)$$

$$\approx \frac{V(\omega)}{\sqrt{2 \left[1 + \left(\frac{Z_s}{Z_0} \right)^2 \right] + 2 \left[1 - \left(\frac{Z_s}{Z_0} \right)^2 \right] \cos[2k(L + cZ_0 C_x)]}} \quad (1b)$$

where $k = \omega/c'$, c , and c' are the speed of light in vacuum and in the transmission line, respectively, Z_0 and Z_s are the line and source impedances, respectively, and Eq. (1b) holds for small $\omega C_x Z_0 \ll 1$.

The behavior of the microscope can be understood from Eq. (1b). For $Z_s \neq Z_0$, the transmission line is mismatched to the source and well-defined standing wave resonances appear on the line. This is the limit in which our system operates. As the probe approaches a conducting part of a sample, C_x increases. From Eq. (1), this is equivalent to the transmission line being lengthened by $cZ_0 C_x$. In normal operation, we apply microwaves at a frequency which is somewhat off resonance. Increasing the length of a transmission line causes all of the resonant frequencies to decrease and V_- to change.

To characterize the system we measured the reflected microwave voltage as a function of frequency and lift-off from a steel surface for the 200 μm inner diameter [see Fig. 2(a), dark represents more reflected power and light less]. The dark vertical bands occur when the source is in resonance with the transmission line. The resonances occur about every 125 MHz, corresponding to $L = 1.1$ m and $c' = 2.61 \times 10^8$ m/s. We note that when the probe is close to the surface, the resonance bands bend toward lower frequencies, corresponding to a reduction of the resonance frequency. The maximum observed (and expected) shift is about 60 MHz, one half of the distance between the resonances, when the probe tip goes from an open condition (far from the sample) to being effectively shorted (C_x large, close to the sample).

Figure 2(a) also shows that the resonance bands wash out when the probe is very close to the surface. This decrease in Q is probably due to the surface resistance of the sample or to radiative losses. In principle, by monitoring the Q , one may be able to directly image microwave losses and perhaps

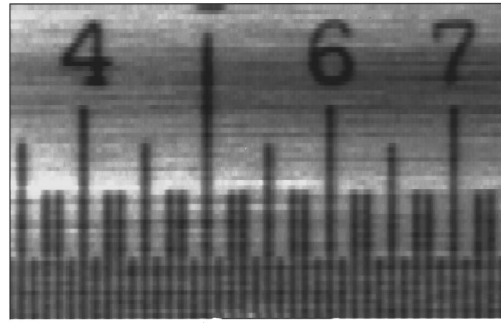


FIG. 3. Microwave scan of Starrett 100-ths in. steel rule at 12.0 GHz using a 100 μm probe. Scan area is 7 by 10 mm. The scanning speed was 1.0 mm/s. The spatial resolution is about 100 μm .

surface resistance. For comparison, Fig. 2(b) shows the reflected voltage calculated from Eq. (1) using a parallel plate approximation for C_x . The bending of the resonance bands is well reproduced by the model.

To investigate the capabilities of the system we image a variety of samples. For example, Fig. 3 shows a reflected microwave image of a Starrett 100-ths in. steel rule taken using the 100 μm probe. This image was taken at 12 GHz with a probe-sample separation of 20 μm . The marks on the rule are indentations approximately 250 μm deep and 120 μm wide. The system easily resolves the marks, with the contrast due to changes in reflected power as the capacitance varies between the probe tip and the sample surface. For this image the rms noise voltage at each pixel is 0.9 μV and the approximate signal strength at a point over one of the grooves is 11 μV . The signal-to-noise ratio, which goes as the square of the voltage, is approximately 150.

To determine the spatial resolution of the system, we scanned a thickness gauge from a Fowler optical comparator using the 100 μm probe. The gauge is a flat 27-mm-diam glass disk with parallel lines made from a thin-film Cr. The lines range in width from 20 to 60 μm [see Fig. 4(a)]. Scanning at 10 GHz and a height of 50 μm , the system was able to detect all the lines [see Fig. 4(b)]. The spatial resolution can be deduced from the image profile of the narrowest lines;

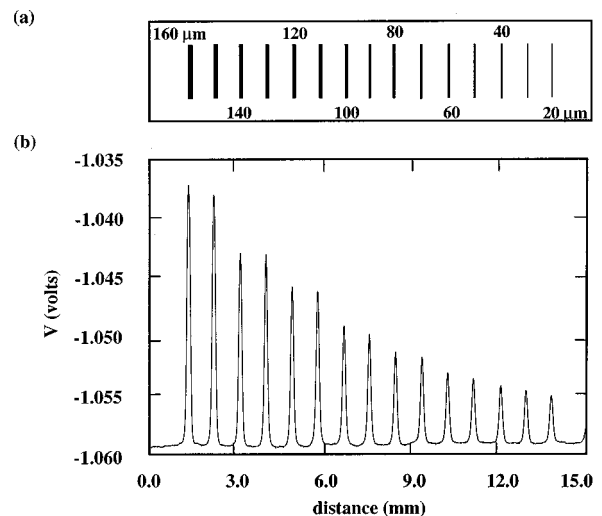


FIG. 4. Scan of thickness gauge reticule from a Fowler optical comparator taken at 10 GHz. There are 15 lines ranging in width from 20–160 μm .

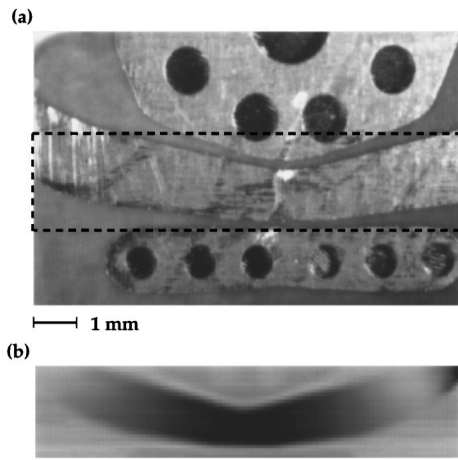


FIG. 5. (a) Photograph of microwave breadboard assembly. Dashed lines show area scanned. (b) Scan of microstrip in receiver mode at 8.50 GHz, with power applied to left end of center strip.

the full width at half maximum of the $20\ \mu\text{m}$ line was $100\ \mu\text{m}$, indicating a spatial resolution of $100\ \mu\text{m}$. From this and similar measurements on other probes, we conclude that the spatial resolution is set by the diameter of the inner conductor of the coax, as expected.

The system can also be used to image active microwave circuits. To do this requires converting the instrument to receiving mode [see dashed line in Fig. 1(a)]. In this configuration the microwave source drives the circuit under investigation and the probe acts as a local microwave pickup. Figure 5(a) shows a photograph of a microstrip line. Figure 5(b) shows the receiver mode image taken using the $200\ \mu\text{m}$ probe with 8.5 GHz microwave power applied to the left end of the strip, an open circuit on the right, and the probe height fixed at $50\ \mu\text{m}$. The resulting image shows a clear standing wave excitation on the microstrip, with an antinode in the center.

In summary, we have constructed a near-field scanning microwave microscope that is based on a short, open-ended, coaxial probe which is coupled to a resonant transmission line. The system operates over a large frequency range and achieves a spatial resolution of $100\ \mu\text{m}$ using simple instrumentation. The spatial resolution is limited by the diameter of the inner wire of the coax, so that finer tips could be used to achieve better spatial resolution.^{12,13} Our system offers several potential advantages over existing systems, including the simplicity of the apparatus and wideband operation (from 0.1 to 50 GHz with appropriate connectors and sources). Ultimately these may allow its use in high-frequency circuit diagnosis, the imaging of surface impedance, and the inspection of large-area wafers.

We thank J. C. Booth for useful discussions and acknowledgment support from the National Science Foundation ECS-9632811, the Center for Superconductivity Research, and one of us (S.M.A.) from NSF NYI Grant No. (DMR-9258183).

¹E. A. Ash and G. Nichols, *Nature (London)* **237**, 510 (1972).

²U. Durig, D. W. Pohl, and F. Rohmer, *J. Appl. Phys.* **59**, 3318 (1986).

³R. J. Gutman, J. M. Borrego, P. Chakrabarti, and M. S. Wang, *IEEE MTT-S Digest*, 281 (1987).

⁴W. Lukosz, *Imagery with Evanescent Waves*, Workshop on Unconventional Imagery (SPIE, Bellingham, WA, 1984), p. 73.

⁵E. A. Ash and A. Husain, *Proceedings of the Fifth European Microwave Conference*, Sept. 1975 (unpublished), p. 213.

⁶T. Wei, X. D. Xiang, W. G. Wallace-Freedman, and P. G. Schultz, *Appl. Phys. Lett.* **68**, 3506 (1996).

⁷J. A. Weiss and D. A. Hawks, *IEEE MTT-S Digest*, 457 (1987).

⁸M. Fee, S. Chu, and T. W. Hansch, *Opt. Commun.* **69**, 219 (1989).

⁹H. A. Bethe, *Phys. Rev.* **66**, 163 (1944).

¹⁰M. Tabib-Azar, N. S. Shoemaker, and S. Harris, *Meas. Sci. Technol.* **4**, 583 (1993).

¹¹S. Ramo, J. R. Whinnery, and T. Van Duzer, *Fields and Waves in Communication Electronics*, 3rd ed. (Wiley, New York, 1994), Chap. 5.

¹²U. Ch. Fisher and M. Zapletal, *Ultramicroscopy* **42-44**, 393 (1992).

¹³H. J. Reitboeck, *J. Neurosci. Methods* **8**, 249 (1983).